

A New Chemical Route for the Synthesis of #- Na_{0.33}V₂O₅ and Its Fully Reversible Li Intercalation

Jae-Kwang Kim, B. Senthilkumar, Sun Hye Sahgong, Jung-Hyun Kim, Miaofang Chi, and Youngsik Kim

ACS Appl. Mater. Interfaces, **Just Accepted Manuscript** • DOI: 10.1021/acsami.5b01260 • Publication Date (Web): 13 Mar 2015

Downloaded from <http://pubs.acs.org> on March 20, 2015

Just Accepted

"Just Accepted" manuscripts have been peer-reviewed and accepted for publication. They are posted online prior to technical editing, formatting for publication and author proofing. The American Chemical Society provides "Just Accepted" as a free service to the research community to expedite the dissemination of scientific material as soon as possible after acceptance. "Just Accepted" manuscripts appear in full in PDF format accompanied by an HTML abstract. "Just Accepted" manuscripts have been fully peer reviewed, but should not be considered the official version of record. They are accessible to all readers and citable by the Digital Object Identifier (DOI®). "Just Accepted" is an optional service offered to authors. Therefore, the "Just Accepted" Web site may not include all articles that will be published in the journal. After a manuscript is technically edited and formatted, it will be removed from the "Just Accepted" Web site and published as an ASAP article. Note that technical editing may introduce minor changes to the manuscript text and/or graphics which could affect content, and all legal disclaimers and ethical guidelines that apply to the journal pertain. ACS cannot be held responsible for errors or consequences arising from the use of information contained in these "Just Accepted" manuscripts.

A New Chemical Route for the Synthesis of β -Na_{0.33}V₂O₅ and Its Fully Reversible Li Intercalation

Jae-Kwang Kim^a, B. Senthilkumar^a, Sun Hye Sahgong^a, Jung-Hyun Kim^{b*}, Miaofang Chi^c,
Youngsik Kim^{a*}

^a School of Energy & Chemical Engineering, Ulsan National Institute of Science and
Technology (UNIST), Ulsan, South Korea

^b Chemical & Materials Systems Laboratory, General Motors Global Research &
Development Center, Warren, Michigan, USA

^c Materials Science & Technology Division, Oak Ridge National Laboratory, Oak Ridge,
Tennessee, USA

*Corresponding authors: junghyun.kim@gm.com (J.H. Kim), ykim@unist.ac.kr (Y. Kim)

Abstract

To obtain good electrochemical performance and thermal stability of rechargeable batteries, various cathode materials have been explored including NaVS₂, β -Na_{0.33}V₂O₅ and Li_xV₂O₅. In particular, Li_xV₂O₅ has attracted attention as a cathode material in Li-ion batteries owing to its large theoretical capacity, but its stable electrochemical cycling (i.e., reversibility) still remains as a challenge and strongly depends on its synthesis methods. In this study we prepared the Li_xV₂O₅ from electrochemical ion-exchange of β -Na_{0.33}V₂O₅, which is obtained by chemical conversion of NaVS₂ in air at high temperatures. Crystal structure and particle morphology of the β -Na_{0.33}V₂O₅ are characterized by using X-ray diffraction (XRD), scanning electron microscopy (SEM) and transmission electron microscopy (TEM) techniques. Energy-dispersive X-ray spectroscopy (EDX) and X-Ray Photoelectron Spectroscopy (XPS), in combination with electrochemical data, suggests that Na ions are extracted from the β -Na_{0.33}V₂O₅ without irreversible structural collapse and replaced with Li ions during following intercalation (i.e. charging) process. Thus obtained Li_xV₂O₅ delivers high discharge capacity of 295 mAh g⁻¹, which correspond to x=2, with crystal structural stability in the voltage range of 1.5 – 4.0 V vs. Li, as evidenced by its good cycling performance and high Coulombic efficiency under 0.1 mA cm⁻² at room temperature. Furthermore, the ion exchanged Li_xV₂O₅ from the β -Na_{0.33}V₂O₅ shows stable electrochemical behavior without structural collapse even at a case of deep discharge to 1.5 V vs. Li.

Keywords: β -Na_{0.33}V₂O₅, Chemical switch, Vanadium sulfides, Vanadium oxides, structural collapse, High capacity cathode.

1. Introduction

Vanadium pentoxide, V_2O_5 , was one of the first oxides to be studied for use as a cathode in lithium ion batteries because its structure consists of VO_5 square pyramids layers with an open Li intercalation site between the layers. The open structure could combine with the wide range of oxidation states for vanadium, which allows for a high theoretical specific capacity of 442 mA h g^{-1} for $\text{Li}_x\text{V}_2\text{O}_5$ at $x=3$. In addition, vanadium is abundant in the crust of earth, guaranteeing the availability and low cost of V_2O_5 .¹⁻³ However, vanadium pentoxide has suffered from poor specific capacity and cycleability due to its low diffusion coefficient of lithium ions and irreversible structural change when Li insertion is more than $x=1$.⁴⁻⁶ Great effort has been made over the last twenty years to improve the phase reversibility of $\text{Li}_x\text{V}_2\text{O}_5$ (*e.g.*, $0 \leq x \leq 2$) by influencing the compound's structure and surface defects as well as its particle size and morphology, which has been created by various synthesis methods and post-treatment conditions.⁷⁻¹²

One of the trials found that a better stable and rigid 3D framework structure with a tunnel was achieved by doping with metallic species (such as Na) into the V_2O_5 , producing $\beta\text{-Na}_{0.33}\text{V}_2\text{O}_5$.^{13,14} The $\beta\text{-Na}_{0.33}\text{V}_2\text{O}_5$ contains three different open intercalation sites (M1-M3) in its 3D tunnel structure where Li can be reversibly intercalated at the range of $0.0 \leq x \leq 1.66$. And, the phase transformations observed in the $\text{Li}_x\beta\text{-Na}_{0.33}\text{V}_2\text{O}_5$ are reversible during cycling, which provide the specific capacity up to 234 mA h g^{-1} at $x = 1.66$. Many types of synthesis methods for the $\beta\text{-Na}_{0.33}\text{V}_2\text{O}_5$, which include solid-state reaction,^{15,16} flux method,¹⁷ sol-gel method,¹⁸⁻²⁰ and hydrothermal method,^{14,21-23} has been attempted to enhance its electrochemical performances. Recent report based on hydrothermal synthesized $\beta\text{-Na}_{0.33}\text{V}_2\text{O}_5$ shows high capacity of 339 mA h g^{-1} and structure stability at depth discharge of 1.5 V .²³

Herein, we primarily reported the chemical switching from NaVS₂ to β -Na_{0.33}V₂O₅ and investigated the structure and phase evolution underlying the lithiation/delithiation process of β -Na_{0.33}V₂O₅, which is critical for improving electrochemical properties. In this work, the β -Na_{0.33}V₂O₅ was synthesized via a new chemical route involving a chemical switch of the NaVS₂ heat-treated at 600 °C in air atmosphere for the first time. The Na ions of the β -Na_{0.33}V₂O₅ were extracted from the compound's structure and Li_xV₂O₅ is prepared by electrochemical ion exchange. The subsequent intercalation of Li ions into Li_xV₂O₅ was observed with $0.0 \leq x \leq 2.0$ without irreversible phase change. To the best of our knowledge, the Na extraction from the Na_{0.33}V₂O₅ has not reported elsewhere and the more inserted lithium ions (x=2) than 1.66 Li into the Na_{0.33}V₂O₅ achieve higher capacity which is beneficial to obtaining high energy density.

2. Experimental section

2.1. Preparation of the samples

To prepare the NaVS₂, appropriate amounts of Na₂S (Sigma, 99%), vanadium (Alfa, 99.5%), and sulfur (Sigma, 99.99%), respectively, were mixed altogether and placed in a carbon-coated quartz tube inside an Ar glove box. Then, the quartz tube was sealed under vacuum. The sealed tube was slowly heated over 20 h to 700 °C, next kept for 40 h at 700 °C, and then slowly cooled over 5 h to 250 °C, followed by quenching the tube in air. While inside an Ar glove box, the samples were removed from the tubes and then thoroughly ground and pelletized. Because the NaVS₂ is sensitive to moisture, it was always handled in an Ar atmosphere.

To prepare the vanadium oxides, the NaVS₂ powders that were loaded in an Al₂O₃ crucible and then placed into the furnace in atmospheric air. The powders were slowly heated

over 5 h to reach 400 °C, 500 °C and 600 °C, respectively, and held for 10 h at each of these temperatures, followed by allowing them to naturally cool to room temperature.

2.2. Structural analysis

The powder x-ray diffraction (XRD) data was collected using the Bruker D8 Advanced diffractometer equipped with Cu-K α radiation and a diffractometer monochromator that was operated at 40 kV and 40 mA. The samples were finely ground and placed in the sample holder of the diffractometer. Data for Rietveld structure refinement were gotten in the 2 θ range 15-120° with 0.02° step interval and 10 second step time. The sample was rotated at 30 rpm during data collection to minimize any preferred orientation and statistical errors in calculation. The crystal structure was refined in the space group *C2/m* using the program GSAS. The morphology of the sample particles were analyzed by scanning electron microscopy (SEM), and the particle surfaces were further characterized using transmission electron microscopy (TEM). The TEM microscope was an aberration-corrected JEOL JEM-2100F operated at 200kV. Samples were made suitable for TEM observation by grinding the heat-treated material into fine powders and dusting them onto lacy-carbon coated copper TEM grids.

2.3. Electrochemical analysis

The electrode and cell were prepared in an Ar glove box. The electrodes were fabricated from a 70:20:10 (wt%) mixture of active material, acetylene black as current conductor, and poly (tetrafluoroethylene) as binder. The mass, diameter and thickness of typical electrode were 10 mg, 7 mm and 0.06 mm, respectively. The electrochemical cells were prepared with standard 2016 coin cell hardware, using Li metal foil as both the counter and reference electrodes. The electrolyte used for analysis was 1 M LiPF₆ in 1:1 EC:DEC. The sealed cells were taken out of the Ar glove box and placed in a battery testing system.

Electrochemical performance tests were carried out using an automatic galvanostatic charge-discharge unit, WBCS 3000 battery cyler, between 1.5 and 4.0 V at room temperature. The experiments were carried out at 0.1 mA cm^{-2} current density. The cells were then aged for 5 h before the first discharge (or charge) to ensure full absorption of the electrolyte into the electrode.

3. Result and Discussions

3.1. Chemical and structural characterizations

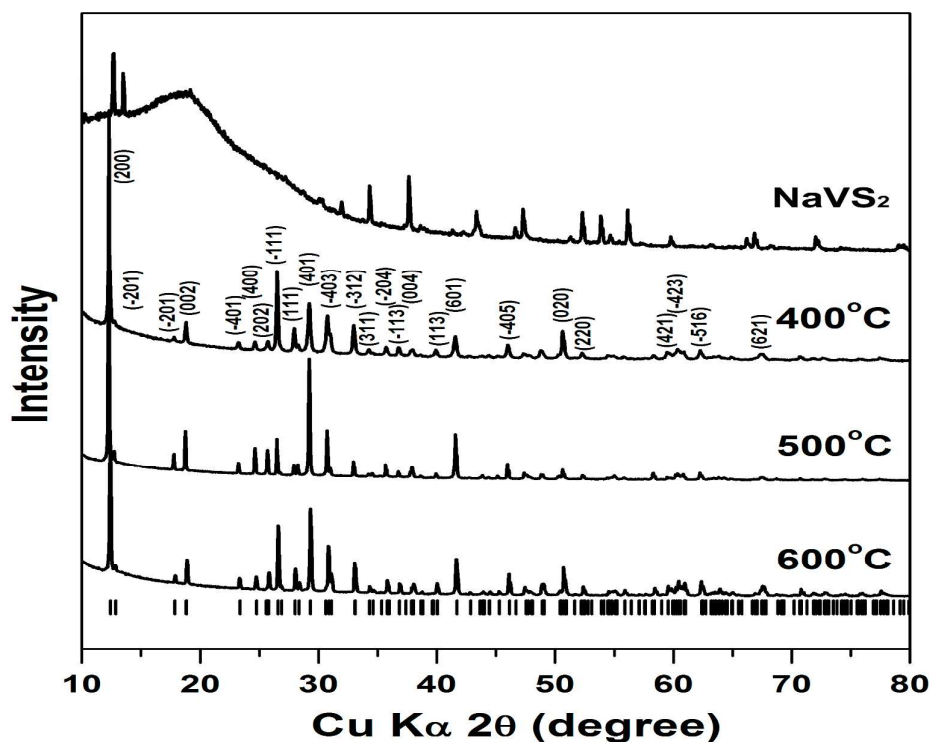


Figure 1. Powder XRD patterns for NaVS_2 and its samples that were heat-treated for 10 h in air at different temperatures with crystal structure of layered NaVS_2 and three dimensional framework $\beta\text{-Na}_{0.33}\text{V}_2\text{O}_5$

This study takes a unique approach to synthesizing a high quality sodium vanadium bronze, $\beta\text{-Na}_{0.33}\text{V}_2\text{O}_5$, with enhanced crystallinity, via the chemical switch of NaVS_2 heat-

1
2
3
4 treated in air. The pristine NaVS₂ sample has the hexagonal structure, consisting of
5
6 hexagonal-close-packed sulfur with V and Na atoms in alternate octahedral-site (001) planes
7
8 forming a layered structure.^{2,3} The XRD patterns of the NaVS₂ sample (Figure 1) matched
9
10 well to those reported in the literature, and such details of their crystal structures were
11
12 discussed.^{2,3}
13

14
15 When the NaVS₂ sample was exposed to atmospheric air and heated at high
16
17 temperature at 600 °C for 10 h, the initial sulfide phase became the mixtures of Na₂SO₄ and
18
19 β-Na_{0.33}V₂O₅ as identified by the XRD (see, Figure S1). The Na₂SO₄ was produced as a result
20
21 of NaVS₂ decomposition during heat-treatment in air, and could be eliminated by washing
22
23 with water as shown in Figure S1. Therefore, heat-treated samples were washed with water to
24
25 remove the Na₂SO₄ phase before further analyses. Figure 1 shows XRD patterns of the
26
27 washed samples. The XRD data from all three samples (400 °C, 500 °C, and 600 °C) can be
28
29 indexed based on the β-Na_{0.33}V₂O₅ phase with a monoclinic symmetry (space group: *C2/m*),
30
31 which has a three-dimensional tunneling structure along the [010] direction.¹⁸⁻²⁰ The results
32
33 of Rietveld refinement obtained from a least-square fitting of the XRD data are summarized
34
35 in Table S1. These results indicate that the chemical and phase transformations of NaVS₂
36
37 toward β-Na_{0.33}V₂O₅ appeared by air oxidation of the NaVS₂ at temperatures in the range of
38
39 400 °C - 600 °C. However, 600 °C calcined sample showed highly crystallinity with a
40
41 formation of high temperature monoclinic β-Na_{0.33}V₂O₅ phase. It also presented typical
42
43 electrochemical voltage profiles (see, Figure S2) of the β-Na_{0.33}V₂O₅ phase, which agrees
44
45 well with literature data.^{18,23} Therefore, further characterizations were performed for the
46
47 600 °C calcined sample.
48
49
50
51
52
53

54 Figure 2 shows the crystal structures determined by the Rietveld refinement for the β-
55
56 Na_{0.33}V₂O₅ (Figure 2a). Sodium vanadium bronze, β-Na_{0.33}V₂O₅ has a monoclinic structure,
57
58
59
60

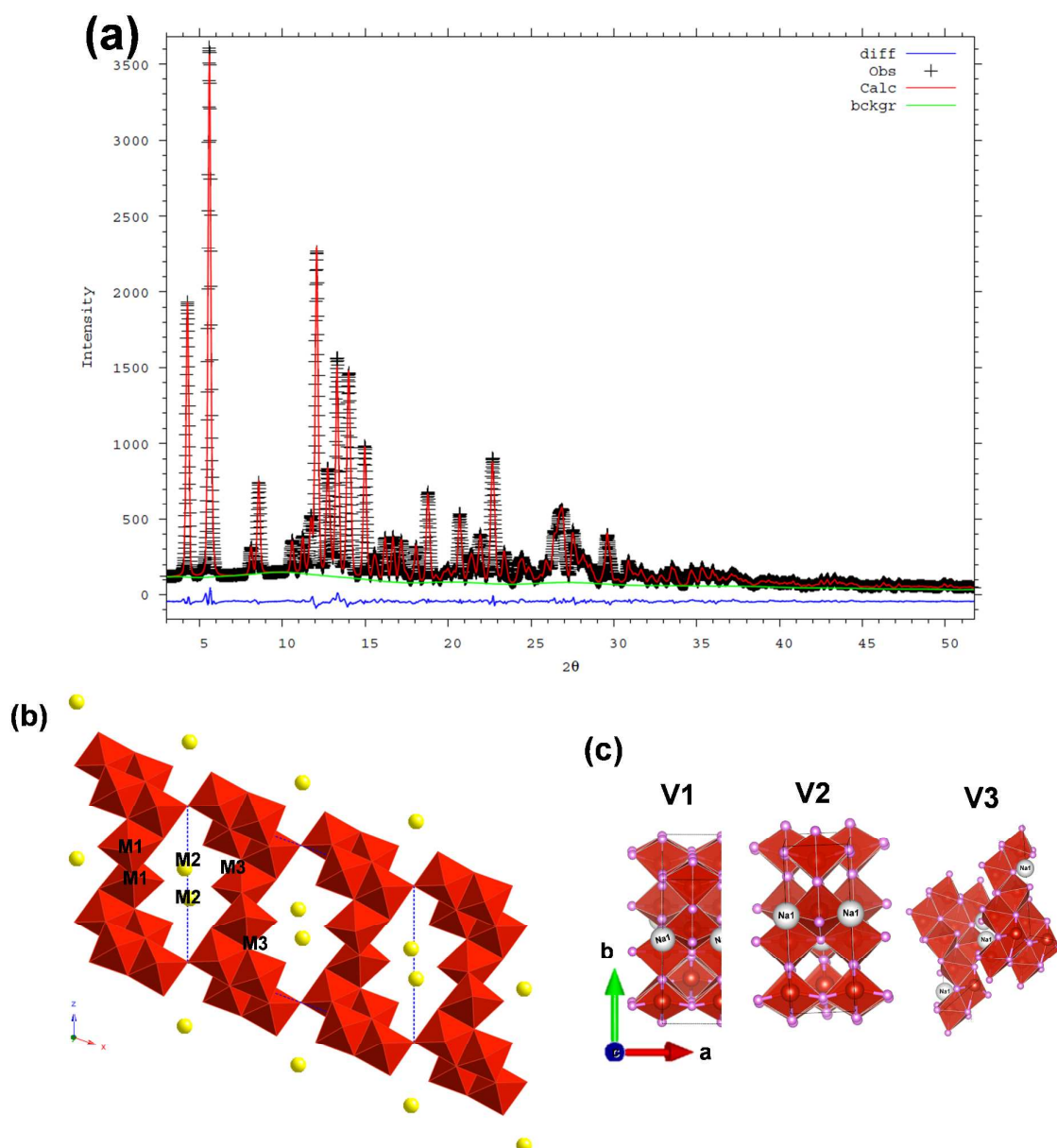


Figure 2. (a) X-ray diffraction pattern and Rietveld refined result of $\beta\text{-Na}_{0.33}\text{V}_2\text{O}_5$. (b) Projection of the crystal structure of $\beta\text{-Na}_{0.33}\text{V}_2\text{O}_5$ on the a - c plane and possible positions (M1-M3) of the inserted cations and (c) Structural subunits of $\beta\text{-Na}_{0.33}\text{V}_2\text{O}_5$: zigzag chains of edge-sharing (V1) O_6 octahedra; two-leg ladders of corner-sharing (V2) O_6 octahedra; zigzag chains of (V3) O_5 polyhedra.

the same as LiV_2O_5 (JCPDS#73-1670). However, the radius of sodium ion is much larger than that of lithium ion. Thus, $\beta\text{-Na}_{0.33}\text{V}_2\text{O}_5$ possesses a larger interlayer distance ($\text{Na}_{0.33}\text{V}_2\text{O}_5$ is 7.06 Å, $\text{Li}_x\text{V}_2\text{O}_5$ is 6.36 Å), a higher lithium diffusion coefficient as well as reduced interaction between the interlayer cations.²⁴ Moreover, the volume change of $\text{Na}_{0.33}\text{V}_2\text{O}_5$ during the Li-ion insertion/extraction processes is smaller. Therefore, $\beta\text{-Na}_{0.33}\text{V}_2\text{O}_5$ has the potential to show improved cyclic performance and rate capability.

Although the $\beta\text{-Na}_{0.33}\text{V}_2\text{O}_5$ prepared by our chemical switch method is the same structure as monoclinic (C2/m space group), the crystal density is higher, lattice parameter of *a*-axis is shorter, and *c*-axis is longer (see, Table 1) than the published data for typical $\beta\text{-Na}_{0.33}\text{V}_2\text{O}_5$. The difference can be found from (V3)O6 octahedra (atomic labels and their corresponding locations are described in Table S1); the (V3)O6 octahedra of our chemically switched $\beta\text{-Na}_{0.33}\text{V}_2\text{O}_5$ grows toward *z*-direction, whereas reported data from typical $\beta\text{-Na}_{0.33}\text{V}_2\text{O}_5$ showed its growth toward (*y,z*)-direction (Figure 2b).²⁴ We speculate that this octahedral growth toward *z*-direction can provide a pillar effect and may be beneficial to maintain stable electrochemical performance without structural collapse during lithiation down to 1.5 V, which is similar to the recently reported on mesoporous $\beta\text{-Na}_{0.33}\text{V}_2\text{O}_5$.²³

Table 1. Structural parameters of powder $\beta\text{-Na}_{0.33}\text{V}_2\text{O}_5$ samples.

Heating Temp.	Phase	Space group	a (Å)	b (Å)	c (Å)	β (degree)	Unit cell volume (Å ³)
400°C	$\beta\text{-Na}_{0.33}\text{V}_2\text{O}_5$	C2/m	10.072	3.609	15.381	109.552	526.80
500°C	$\beta\text{-Na}_{0.33}\text{V}_2\text{O}_5$	C2/m	10.068	3.608	15.343	109.378	525.77
600°C	$\beta\text{-Na}_{0.33}\text{V}_2\text{O}_5$	C2/m	10.068	3.607	15.387	109.556	526.59

As shown in Figure 2b the $\beta\text{-Na}_{0.33}\text{V}_2\text{O}_5$ bronzes crystallizes in a monoclinic tunnel-like structure, space group C2/m with Z=6 formula units per unit cell. In the crystal structure a

characteristic ladder-like V_2O_5 host framework is formed by edge/corner sharing of VO_6 octahedra and VO_5 square pyramids.^{17,18} There are three structural units with three different sites for vanadium atoms, V_1 is coordinated with six oxygen forms $V_1(O_6)$ octahedra which build zigzag double-chain by sharing edges, $V_2(O_6)$ octahedra form a ladder chain by sharing corners and V_3 sites have 5-fold square pyramidal coordination forms $(V_3)O_5$ polyhedron (Figure 2c).¹⁷ Vanadium-centered polyhedrons in one layer form zigzag double-chains which construct the three dimensional network along b -axis. The V_2O_5 host framework gives rise to unidirectional tunnel along the crystallographic b -axis in which the Na ions are inserted.

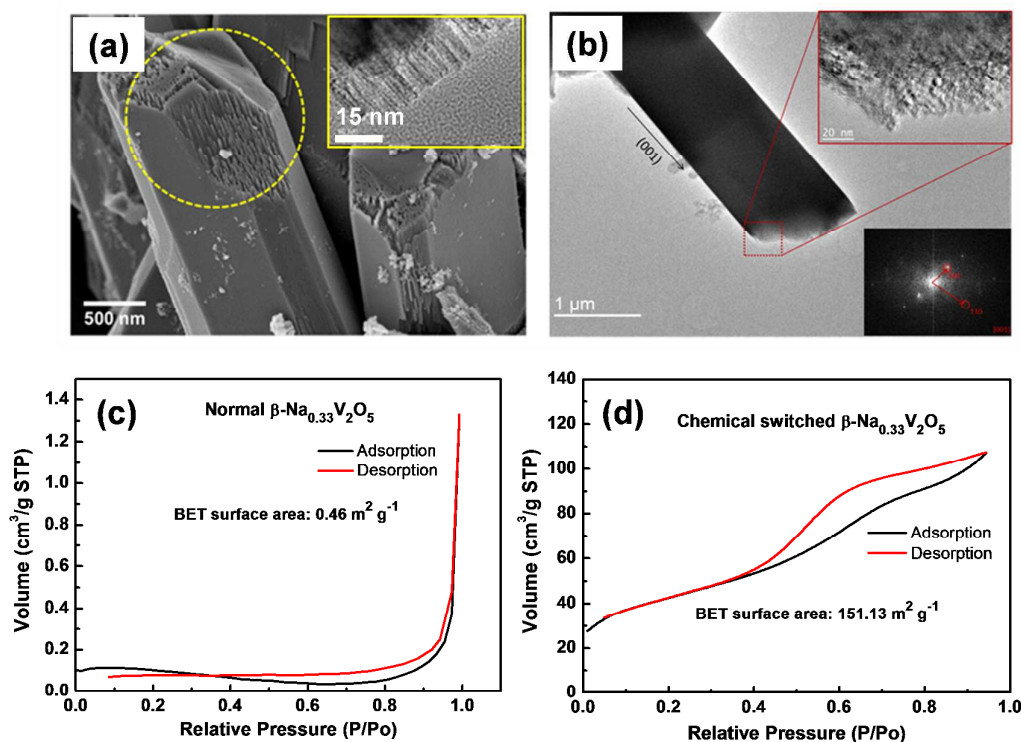


Figure 3. The crystal defects were observed on the surface of the rod-shaped crystals, as circled in yellow in (a), where high-resolution SEM image was taken. (b) TEM image of a rod-shaped particle of the $\beta\text{-Na}_{0.33}\text{V}_2\text{O}_5$, which reveals that the longitudinal surface of the particle is (001), and a considerable amount of stacking faults exist parallel to this face. Nitrogen sorption isotherms and mesopore size distributions in the general $\beta\text{-Na}_{0.33}\text{V}_2\text{O}_5$ (c) and the chemically switched $\beta\text{-Na}_{0.33}\text{V}_2\text{O}_5$ (d).

Highly anisotropic quasi-one dimensional conductivity of the tunnel is owing to the partial reduction of V_2O_5 framework.²⁵ Na ions are located in four interstitial sites per unit cell along b axis (M_1). The tunnel structure of β - $Na_{0.33}V_2O_5$ bronze has two additional tunnel sites for Li intercalation; four eight-coordinated sites M_2 and four tetrahedral sites M_3 per unit cell (Figure 2b).²³⁻²⁵ Atomic positions and thermal factors are gathered in Table S1.

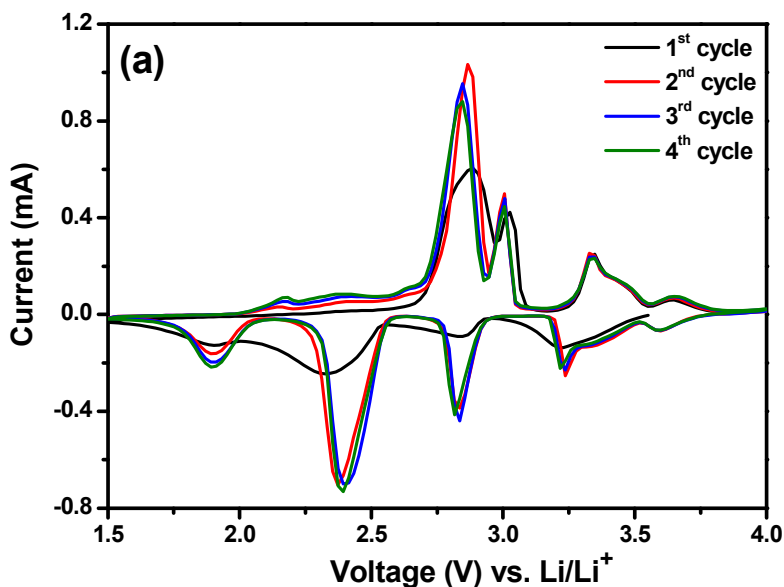
A high magnification SEM image shows that the β - $Na_{0.33}V_2O_5$ was well crystalized and rod-shaped with a length of 7–15 μm and a width of 1–3 μm as shown in Figure 3a. The 600 °C sample particles have surface defects in the shape of crystals around the edges of the particles, which exposes layers of grains (highlighted with a yellow dotted line). The high-resolution TEM image in Figure 3b also shows the layered grains along the crystal defects. The TEM image reveals that the longitudinal surface of the rod-shaped particle is parallel to (001) where a considerable amount of stacking faults exist at particle edges. It is plausible that the growth of the rod-shaped β - $Na_{0.33}V_2O_5$ crystals could be interfered by co-existing Na_2SO_4 salt crystals at the edge (or surface) area during heat-treatment at 600 °C. The surface defects could be exposed after removing Na_2SO_4 by washing the sample in water.

The unique crystal defects induce increase of surface area and the fairly large porous nature of the chemical switched β - $Na_{0.33}V_2O_5$ as compared to the sol-gel synthesized β - $Na_{0.33}V_2O_5$, which is also supported by the data from the BET surface area measurements (Figure 3c, d). The surface area of the chemically switched β - $Na_{0.33}V_2O_5$ is higher, while the average pore size decreases. Thus, the average pore size and surface area of the composite particles largely depend on the synthetic process, as chemically switched β - $Na_{0.33}V_2O_5$ has the largest surface area and the highest number of pores. This can contribute to shorten diffusion path of Li^+ ions and offer more active sites for electrochemical reactions, and furthermore a capacious container for electrolyte penetration into internal phases and a rigid

scaffold to release the negative volumetric force from extraction and insertion process of lithium ions.

3.2 Electrochemical characterizations of the samples

Cyclic voltammograms of $\beta\text{-Na}_{0.33}\text{V}_2\text{O}_5$ recorded at a scan rate of 0.1 mV s^{-1} are shown in Figure 4a. Well defined oxidation/reduction peaks were observed in the CV curves. The cathodic peaks observed at 3.24, 2.82, 2.38 and 1.88 V are belongs to the multiple-step intercalation of lithium-ions into the $\beta\text{-Na}_{0.33}\text{V}_2\text{O}_5$ phase. Similarly, de-intercalation of lithium-ions from the $\beta\text{-Na}_{0.33}\text{V}_2\text{O}_5$ phase was identified by anodic peaks at 2.17, 2.85, 3.02 and 3.34



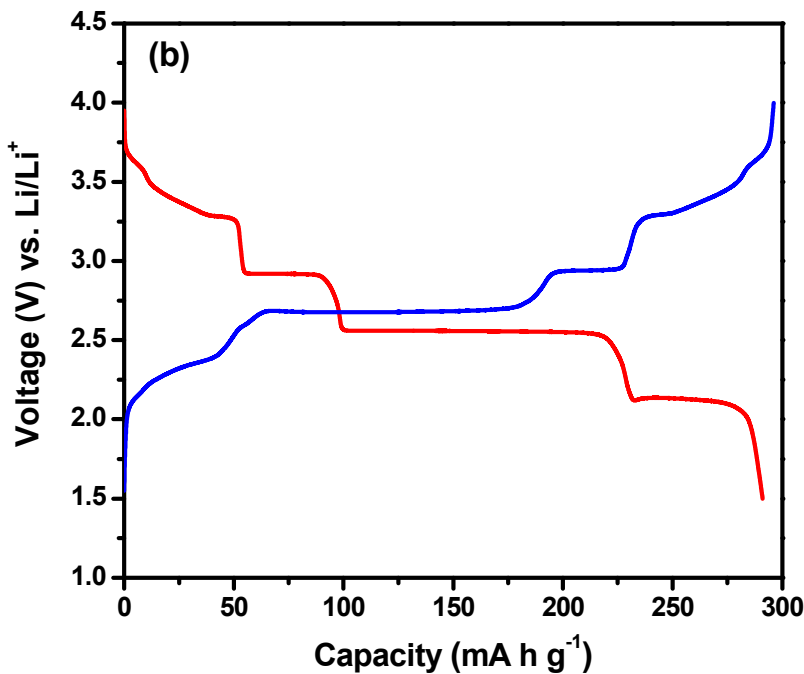


Figure 4. (a) Cyclic voltammograms (CV) of $\beta\text{-Na}_{0.33}\text{V}_2\text{O}_5$ at a scan rate of 0.1 mV s^{-1} and (b) Charge-discharge curve of $\beta\text{-Na}_{0.33}\text{V}_2\text{O}_5$ at a current density of 0.1 mA cm^{-2} .

V .^{23,25} Charge-discharge curves of $\beta\text{-Na}_{0.33}\text{V}_2\text{O}_5$ recorded at a current density of 0.1 mA cm^{-2} are shown in Figure 4b. The four distinct voltage steps were observed at $\sim 3.3\text{ V}$, $\sim 2.9\text{ V}$, $\sim 2.5\text{ V}$, and $\sim 2.1\text{ V}$ during the Li insertion into the $\beta\text{-Na}_{0.33}\text{V}_2\text{O}_5$ phase which is consistent with the CV results. The first three voltage profiles located at 3.3 V , 2.9 V , and 2.5 V were assigned to the Li ion occupancy of the $\beta\text{-Na}_{0.33}\text{V}_2\text{O}_5$ structure's particular empty sites, M3, M2, and M1, respectively (Figure 2b).⁴ The Na ions were initially located at the M1 sites of the $\beta\text{-Na}_{0.33}\text{V}_2\text{O}_5$ structure. During the discharging of the cell, when the voltage was 3.3 V , the Li ions began to occupy the M3 sites of the $\beta\text{-Na}_{0.33}\text{V}_2\text{O}_5$ structure when $0 < x \leq 0.33$. The second voltage step at 2.9 V was assigned to the half-occupancy by the Li ions of the M2 sites when $0.33 < x \leq 0.66$.²⁵ And finally, the large voltage plateaus at 2.5 V was assigned to the filling of the

1
2
3
4 remaining M1, M2, and M3 sites by the Li ions when $0.66 < x \leq 1.67$.²⁵ Such Li ion
5
6 distribution to the M sites was reported to be thermodynamically and kinetically more
7
8 favorable by minimizing the ion-ion repulsive Coulombic interactions during Li insertion into
9
10 the $\beta\text{-Na}_{0.33}\text{V}_2\text{O}_5$ structure.⁴ During Li insertion into the $\beta\text{-Na}_{0.33}\text{V}_2\text{O}_5$, the Na ions of its
11
12 structure were reported to be very stable even at higher temperature range (100 - 450 °C).⁶ As
13
14 a result, the degree of Li insertion into the $\beta\text{-Na}_{0.33}\text{V}_2\text{O}_5$ structure is 1.67, but the total number
15
16 of intercalated ions in the structure is 2 ($0.33\text{Na} + 1.67\text{Li}$).
17
18

19
20 To confirm the electrochemical extraction of Na from the $\beta\text{-Na}_{0.33}\text{V}_2\text{O}_5$ structure, the cell
21
22 was charged first to 4.0 V (see Figure 5a). The charge voltage curve was observed at ~3.3 V,
23
24 and its capacity (47 mA h g^{-1}) corresponds well to the 0.33 Na per unit formula. The
25
26 following discharge was performed to observe Li insertion into the structure. However, to
27
28 eliminate the possibility of Na re-insertion into the structure, the Na-extracted electrode was
29
30 collected after charging the cell and washed in DEC. This electrode was placed in the fresh
31
32 coin cell with a Li metal anode and a 1 M LiPF_6 in EC:DEC electrolyte, which was
33
34 discharged first to 1.5 V, as shown in Figure 5a. In addition to the reported three voltage steps
35
36 at ~ 3.3 V, ~2.9 V, and ~2.5 V, a fourth voltage plateau was observed at 2.1 V when the cell
37
38 was discharged to 1.5 V.
39
40
41
42
43
44
45
46
47
48
49
50
51
52
53
54
55
56
57
58
59
60

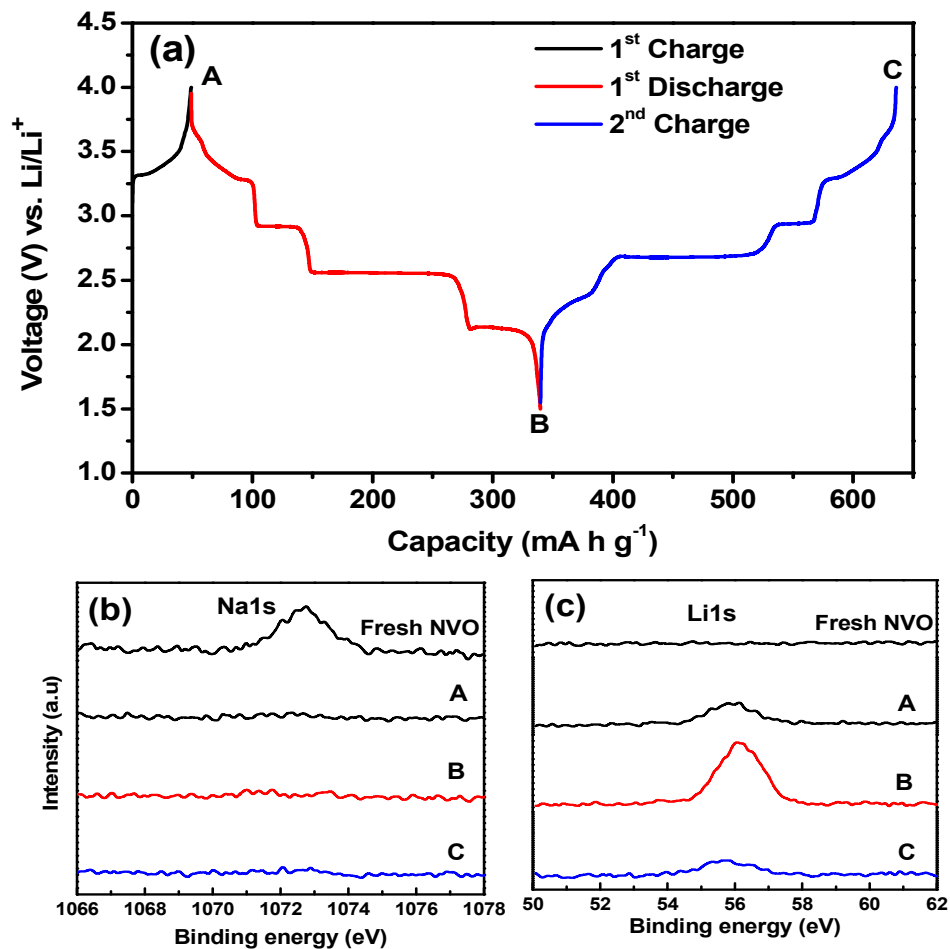


Figure 5. (a) The galvanostatic charge-discharge curve of $\beta\text{-Na}_{0.33}\text{V}_2\text{O}_5$ (NVO) (A is after first charge, B is after first discharge and C is after second charge). Ex-situ XPS of Na 1s (b) and Li 1s (c).

From these results, it can be expected that the Na ions are extracted from the $\beta\text{-Na}_{0.33}\text{V}_2\text{O}_5$ during the charge process, and more Li ions are inserted into its structure during discharge process, which results in the capacity increase after five cycles. Hence, the voltage step at 2.1 V can be related to the substitution of Na ions by Li ions in the $\beta\text{-Na}_{0.33}\text{V}_2\text{O}_5$ structure. So, The 5 well-defined Li insertion processes (the ~ 3.3 sloped curve, the 2.9 V and 2.5 V, as well as 2.1 V potential plateaus) are connected with the Li contents range of

$0 < x \leq 0.33$, $0.33 < x \leq 0.66$, $0.66 < x \leq 1.67$ and $1.67 < x \leq 2.0$, respectively. This is in good accordance with the previous result that $\beta\text{-Li}_x\text{V}_2\text{O}_5$ was kept throughout a rather large voltage range of 1.5 V-4.5 V cut-off.²⁶⁻²⁸

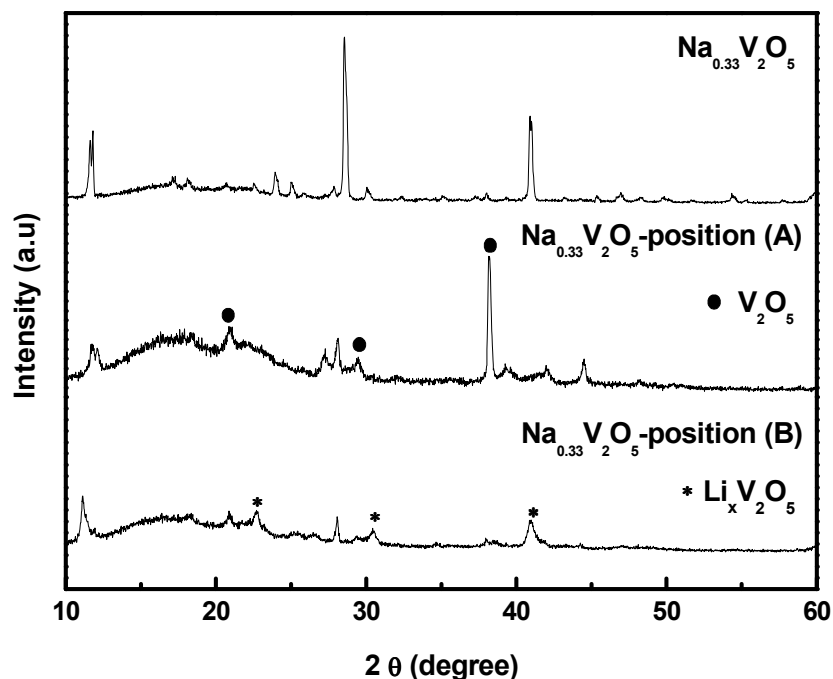


Figure 6. Ex-situ XRD patterns of fresh, charged (A) and discharged (B) $\beta\text{-Na}_{0.33}\text{V}_2\text{O}_5$ electrodes.

The ex-situ XPS and EDX measurements of Figure 5b, c and Figure S3 clearly demonstrate the Na ion extraction and Li ion insertion during charge-discharge process. These results were consistent with the XPS and EDX measurement collected from the fresh electrode of the $\beta\text{-Na}_{0.33}\text{V}_2\text{O}_5$, the first charged electrode to 4.0 V (position A), the first discharged electrode to 1.5 V (position B) and the second charged electrode to 4.0 V again (position C). The $\beta\text{-Na}_{0.33}\text{V}_2\text{O}_5$ electrodes were carefully disassembled and washed by DEC and then investigated by XPS and SEM-EDX. Figure 5b, c shows the high resolution XPS core level spectra of Na1s and Li1s. After first charge, the signal of Na1s disappears and do not appears again. This is indicating that Na ion is extracted during first charge and Li ion is

filled in the vacant of Na ion during discharge (position B). The amount of Li1s peak at position (A) and (C) is the same and that is influence of lithium salt, which place on the surface of electrode. The signal of Li1s at position B of discharged $\beta\text{-Na}_{0.33}\text{V}_2\text{O}_5$ much increase due to insertion of Li ions into M sites (Figure 5c). The amount of Na content in the EDX of the charged $\beta\text{-Na}_{0.33}\text{V}_2\text{O}_5$ electrode was significantly low compared with that of the fresh electrode as shown in Fig. 4d, which corresponds with XPS result. Na is not found into $\beta\text{-Na}_{0.33}\text{V}_2\text{O}_5$ particles at position A, B and C by sodium SEM-mapping (Figure S4). Also, ex-situ XRD patterns display the structure change with extraction of Na ion and insertion of Li ion (Figure 6). The $\beta\text{-Na}_{0.33}\text{V}_2\text{O}_5$ is transformed as V_2O_5 by extraction of Na ions at position A. XRD pattern of recharged electrode (position C) shows $\text{Li}_x\text{V}_2\text{O}_5$ monoclinic structures with insertion of lithium ions.

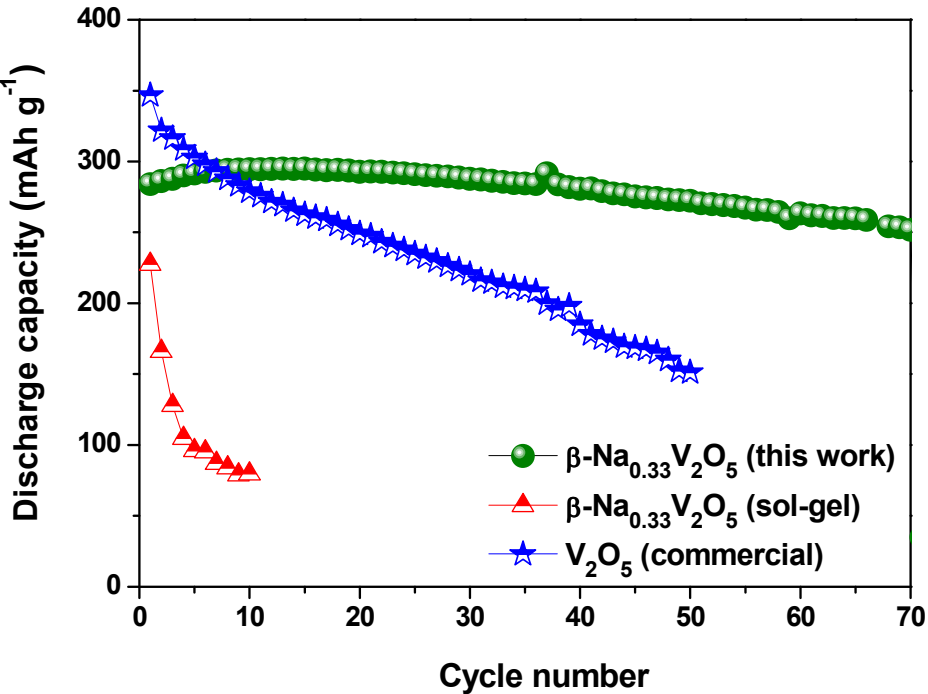


Figure 7. The cycling performance of the $\beta\text{-Na}_{0.33}\text{V}_2\text{O}_5$ measured at the current rate of 0.1 mA cm^{-2} (cut-off: 4.0 V-1.5 V, room temperature).

The chemical switched $\beta\text{-Na}_{0.33}\text{V}_2\text{O}_5$ showed in Figure 7 that the specific capacity of 284 mA h g⁻¹ (after 1st discharging to 1.5V) was increased to 295 mA h g⁻¹ (after 10th discharge) that corresponds to $x = \sim 2.0$ in $\text{Li}_x\beta\text{-Na}_{0.33}\text{V}_2\text{O}_5$. Impedance spectra for $\beta\text{-Na}_{0.33}\text{V}_2\text{O}_5$ at 1st and 10th cycles are shown in Figure S4(a). All three curves show semicircle in the high frequency region and inclined line in the low frequency region. The semicircle is assigned to the formation of solid electrolyte interface (SEI) and creates impedance at the surface of the electrode particles in contact with the organic electrolyte.^{23,29} The increase in impedance observed in the first cycle is due to the development of the passivation film at the Li metal surface.³⁰ When increasing cycles high frequency arc get decreased which indicates the decrease in charge-transfer resistance. The lithium-ion diffusion coefficient (D) can be obtained from either the 45° portion of the line or from equations (1) and (2).^{31,32}

$$D = \frac{R^2 T^2}{2n^4 F^4 C^2 \sigma^2} \quad (1)$$

where R is the gas constant, T is the temperature, n is the number of electrons per molecule during oxidization, F is the Faraday constant, C is the concentration of lithium ion, and σ is the Warburg factor. The Warburg factor σ can be obtained from equation (2):

$$Z'' = \frac{\sigma \omega}{2} \quad (2)$$

Figure S4(b) shows the relationship between Z'' and square root of frequency ($\omega^{-1/2}$) in the low-frequency region for $\beta\text{-Na}_{0.33}\text{V}_2\text{O}_5$ electrodes. The calculated lithium ion diffusion coefficient for fresh electrode is $1.3 \times 10^{-15} \text{ m}^2 \text{ s}^{-1}$ which is increased to $4.1 \times 10^{-15} \text{ m}^2 \text{ s}^{-1}$ for cycled electrode. The capacity and voltage plateaus observed in the discharge process are very reversible during the charge process (Figure S5). Since the maximum number of Li ions that can be inserted into the $\beta\text{-Na}_{0.33}\text{V}_2\text{O}_5$ is $x = 1.67$, it could be expected that the extra number of $x = 0.33$ correlates to the Li ions replacing the Na ions located at the M1 sites. This was also observed in the recent electrochemical study of the $\beta\text{-Na}_{0.33}\text{V}_2\text{O}_5$ nanorods,²²

where more than 1.6 Li intercalation into its nanorod structure was observed while extracting Na from the structure when the cell was discharged to 1.5 V. The comparative charge-discharge profile of chemically switched $\beta\text{-Na}_{0.33}\text{V}_2\text{O}_5$ with commercial V_2O_5 is shown in Figure S5. The electrochemical reaction is fully reversible where $0 \leq x \leq 1.5$ in the general $\beta\text{-Na}_{0.33}\text{V}_2\text{O}_5$, prepared by reported synthesis process.¹⁸⁻²⁰ However, for $x > 1.5$ the electrochemical reaction is no longer reversible when is discharged to below 2.2 V, which is the major reason of poor cycle stability (Figure 7). The electrochemical ion exchanged $\text{Li}_x\text{V}_2\text{O}_5$ display stable cycle performance to 70 cycles, even depth discharge to 1.5 V (Figure 7) because the efficient crystal structure and internal pores formed by crystal defect helps fast ions transfer with prevention of crystal collapse. The $\text{Li}_x\text{V}_2\text{O}_5$ retains 89 % capacity after 70 cycles with 99 % Coulombic efficiency. However the slight capacity fading observed is due to the slow lithium ions diffusion for intercalation/deintercalation.^{23,28}

To the best of our knowledge, this is the first time work that reports the Na ions extraction from the $\beta\text{-Na}_{0.33}\text{V}_2\text{O}_5$ without irreversible structural change and further reversible Li ions intercalation into its structure in the range of $0 \leq x \leq 2$. The chemical switch of NaVS_2 heat-treated in air is a typical method to synthesizing a high quality sodium vanadium bronze, $\beta\text{-Na}_{0.33}\text{V}_2\text{O}_5$, with enhanced crystallinity. The 600 °C calcined sample showed high crystallinity with a formation of high temperature monoclinic $\beta\text{-Na}_{0.33}\text{V}_2\text{O}_5$ phase. The stable electrochemical performance of the sample is due to its highly crystalline nature. The high temperature annealing can improve the conductivity which is beneficial for facile electron transportation.³³⁻³⁵ In addition chemically switched $\beta\text{-Na}_{0.33}\text{V}_2\text{O}_5$ showed porous nature and increase in surface area ($151.13 \text{ m}^2 \text{ g}^{-1}$) compared to the sol-gel synthesized $\beta\text{-Na}_{0.33}\text{V}_2\text{O}_5$. The porous structure formed on the surface of the $\beta\text{-Na}_{0.33}\text{V}_2\text{O}_5$ phase and unique crystal structure compared with reported $\beta\text{-Na}_{0.33}\text{V}_2\text{O}_5$ could stabilize the abrupt structural transformation during Li intercalation when cycling, can be expected for the $\beta\text{-Na}_{0.33}\text{V}_2\text{O}_5$

phase reversibility, during cycling.^{23,24,28} The cell parameters of the β -Na_{0.33}V₂O₅ prepared by chemical switch are different with reported β -Na_{0.33}V₂O₅ and *b*-axis is shorter, which is benefit to ion diffusion and prevention of structure collapse.²⁴ Moreover, the high porosity of chemically switched β -Na_{0.33}V₂O₅ plays an important role to achieve high capacity where $x \leq 2$ with depth discharges to 1.5 V without structure collapse.²³

4. Conclusions

The highly crystalline β -Na_{0.33}V₂O₅ was created via a new method of chemical switch, transforming the NaVS₂ sulfide by heat-treatment in atmospheric air. The chemically switched β -Na_{0.33}V₂O₅ showed rod-shaped particles that were 7 – 15 μm long and 1 – 3 μm wide. Also, the β -Na_{0.33}V₂O₅ has unique crystal structure with short *b*-axis cell parameter and crystal defects, allowing high porosity and fast ion diffusion in the internal phase. The β -Na_{0.33}V₂O₅ is converted into Li_{*x*}V₂O₅ by electrochemical ion exchange and enables depth discharge to 1.5 V to achieve high capacity. The ion exchanged Li_{*x*}V₂O₅ delivered a high capacity of 285 mA h g⁻¹ and showed stable cycle performance at a 0.1 mA cm⁻² in a voltage range of 1.5 V–4 V. This electrochemical process corresponds to a reversible insertion/extraction of two Li ($0 \leq x \leq 2$) by extracting Na from the β -Na_{0.33}V₂O₅ structure, although the reported β -Na_{0.33}V₂O₅ is possible to $x=1.67$ with Li_{*x*} β -Na_{0.33}V₂O₅. In addition, ex-situ XPS, SEM-EDX and ex-situ XRD results supported the extraction of Na from the β -Na_{0.33}V₂O₅ structure. The large capacity of this sample is quite attractive in terms of increased energy density for Li ion batteries. The β -Na_{0.33}V₂O₅ micro-sized particle prepared by chemical switch shows good structural reversibility when $0 \leq x \leq 2$, which have not been reported in any other literature.

Acknowledgements

The work performed at UNIST was financially supported by National Research Foundation of Korea (NRF-2014R1A2A1A11052110). Part of the Microscopy research is supported by ORNL's Shared Research Equipment (SHaRE) User Facility that is sponsored by the Office of Basic Energy Sciences, U.S. Department of Energy.

Supporting Information

Supporting Information involves additional XRD pattern, SEM images, SEM–EDX Mapping, Impedance spectra of β -Na_{0.33}V₂O₅ electrodes and electrochemical performance for the NaVS₂ and heat-treated NaVS₂ samples. This information is available free of charge via the Internet at <http://pubs.acs.org/>.

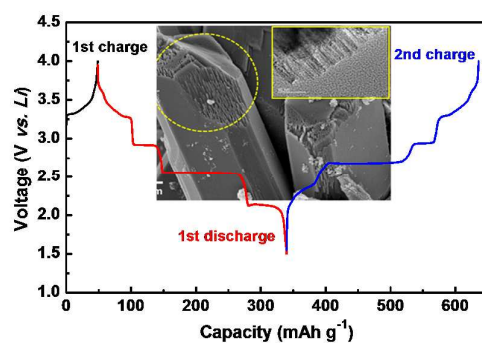
References

- (1) Whittingham, M. S. The Role of Ternary Phases in Cathode Reactions. *J. Electrochem. Soc.* **1976**, *123*, 315–320.
- (2) Delmas, C.; Br  thes, S.; M  n  trier, M. ω -Li_xV₂O₅ — a New Electrode Material for Rechargeable Lithium Batteries. *J. Power Sources* **1991**, *34*, 113–118.
- (3) Cartier, C.; Tranchant, a.; Verdaguer, M.; Messina, R.; Dexpert, H. X-ray diffraction and X-ray absorption studies of the Structural modifications induced by Electrochemical Lithium intercalation into V₂O₅. *Electrochim. Acta* **1990**, *35*, 889–898.
- (4) Cocciantelli, J. M.; Doumerc, J. P.; Pouchard, M.; Broussely, M.; Labat, J. Crystal chemistry of electrochemically inserted Li_xV₂O₅. *J. Power Sources* **1991**, *34*, 103–111.
- (5) Zhai, T.; Liu, H.; Li, H.; Fang, X.; Liao, M.; Li, L.; Zhou, H.; Koide, Y.; Bando, Y.; Golberg, D. Centimeter-long V₂O₅ nanowires: From synthesis to Field-emission, Electrochemical, Electrical transport, and Photoconductive properties. *Adv. Mater.* **2010**, *22*, 2547–2552.
- (6) Mai, L.; Xu, L.; Han, C.; Xu, X.; Luo, Y.; Zhao, S.; Zhao, Y. Electrospun ultralong hierarchical Vanadium oxide nanowires with high performance for Lithium ion batteries. *Nano Lett.* **2010**, *10*, 4750–4755.
- (7) Baddour-Hadjean, R.; Marzouk, a.; Pereira-Ramos, J. P. Structural modifications of Li_xV₂O₅ in a Composite cathode (0 < x < 2) investigated by Raman microspectrometry. *J. Raman Spectrosc.* **2012**, *43*, 153–160.
- (8) Asl, N. M.; Kim, J.-H.; Lee, W. C.; Liu, Z.; Lu, P.; Kim, Y. A new chemical route for the synthesis of β' -Li_xV₂O₅ for use as a high performance cathode. *Electrochim. Acta* **2013**, *105*, 403–411.

- (9) Wang, Y.; Takahashi, K.; Lee, K.; Cao, G. Nanostructured Vanadium oxide electrodes for enhanced lithium-ion intercalation. *Adv. Funct. Mater.* **2006**, *16*, 1133–1144.
- (10) Liu, D.; Liu, Y.; Garcia, B. B.; Zhang, Q.; Pan, A.; Jeong, Y.-H.; Cao, G. V_2O_5 xerogel electrodes with much enhanced Lithium-ion intercalation properties with N_2 annealing. *J. Mater. Chem.* **2009**, *19*, 8789–8795.
- (11) Zhang, X.; Wang, K.; Wei, X.; Chen, J. Carbon-Coated V_2O_5 Nanocrystals as High Performance Cathode Material for Lithium Ion Batteries. *Chem. Mater.* **2011**, 5290–5292.
- (12) Su, D.; Wang, G.; Accepted, J. Single Crystalline Bilayered V_2O_5 Nanobelts for High Capacity Sodium-Ion Batteries. *ACS Nano* **2013**, 11218–11226.
- (13) Gödickemeier, M. Engineering of Solid Oxide Fuel Cells with Ceria-Based Electrolytes. *J. Electrochem. Soc.* **1998**, *145*, 414–421.
- (14) Xu, Y.; Han, X.; Zheng, L.; Yan, W.; Xie, Y. Pillar effect on Cyclability Enhancement for Aqueous Lithium ion batteries: a New Material of β -vanadium bronze $M_{0.33}V_2O_5$ ($M = Ag, Na$) nanowires. *J. Mater. Chem.* **2011**, *21*, 14466–14472.
- (15) Raistrick, I. D. Lithium Insertion Reactions in Tungsten and Vanadium Bronzes. *Solid State Ionics* **1983**, *10*, 425–430.
- (16) Raistrick, I. D. Lithium insertion reactions in oxide bronzes. *Rev. Chim. Min.*, **1984**, *21*, 456–467.
- (17) Rabia, K.; Pashkin, a.; Frank, S.; Obermeier, G.; Horn, S.; Hanfland, M.; Kuntscher, C. A High-pressure XRD study of β - $Na_{0.33}V_2O_5$. *High Press. Res.* **2009**, *29*, 504–508.
- (18) Pereiramos, J.; Messina, R.; Znaidi, L.; Baffier, N. Electrochemical Lithium Intercalation in $Na_{0.33}V_2O_5$ Bronze prepared by Sol-gel Processes. *Solid State Ionics* **1988**, 28-30, 886–894.
- (19) Bach, S. A. Thermodynamic and Kinetic Study of Electrochemical Lithium Intercalation in $Na_{0.33}V_2O_5$ Bronze Prepared by a Sol-Gel Process. *J. Electrochem. Soc.* **1990**, *137*, 1042–1048.
- (20) Kim, Y.; Goodenough, J. B. Reinvestigation of $Li_{1-x}Ti_yV_{1-y}S_2$ Electrodes in Suitable Electrolyte: Highly Improved Electrochemical Properties. *Electrochem. Solid-State Lett.* **2009**, *12*, A73–A75.
- (21) Khoo, E.; Wang, J.; Ma, J.; Lee, P. S. Electrochemical energy storage in a β - $Na_{0.33}V_2O_5$ Nanobelt network and its Application for Supercapacitors. *J. Mater. Chem.* **2010**, *20*, 8368–8374.
- (22) Liu, H.; Wang, Y.; Li, L.; Wang, K.; Hosono, E.; Zhou, H. Facile synthesis of NaV_6O_{15} Nanorods and its Electrochemical behavior as Cathode Material in Rechargeable Lithium batteries. *J. Mater. Chem.* **2009**, *19*, 7885–7891.
- (23) Liang, S.; Zhou, J.; Fang, G.; Zhang, C.; Wu, J.; Tang, Y.; Pan, A. Synthesis of Mesoporous β - $Na_{0.33}V_2O_5$ with Enhanced Electrochemical Performance for Lithium ion batteries. *Electrochim. Acta* **2014**, *130*, 119–126.
- (24) Tang, Y.; Sun, D.; Wang, H.; Huang, X.; Zhang, H.; Liu, S.; Liu, Y. Synthesis and Electrochemical properties of NaV_3O_8 Nano flakes as High-performance Cathode for Li-ion battery. *RSC Adv.* **2014**, *4*, 8328–8334.
- (25) Li, W.D.; Xu, C.Y.; Pan, X.L.; Huang, Y.D.; Zhen, L. High Capacity and Enhanced Structural Reversibility of β - $Li_xV_2O_5$ Nanorods as the Lithium Battery Cathode. *J. Mater. Chem. A* **2013**, *1*, 5361–5369.
- (26) O'Dwyer, C.; Lavayen, V.; Tanner, D. a.; Newcomb, S. B.; Benavente, E.; González, G.; Torres, C. M. S. Reduced surfactant uptake in three dimensional assemblies of

- VO_x Nanotubes Improves Reversible Li⁺ intercalation and charge capacity. *Adv. Funct. Mater.* **2009**, *19*, 1736–1745.
- (27) Jiang, J.; Wang, Z.; Chen, L. Structural and Electrochemical Studies on β-Li_xV₂O₅ as Cathode Material for Rechargeable Lithium Batteries. *J. Phys. Chem. C* **2007**, *111*, 10707–10711.
- (28) Baddour-Hadjean, R.; Bach, S.; Emery, N.; Pereira-Ramos, J. P. The peculiar structural behaviour of β-Na_{0.33}V₂O₅ upon electrochemical lithium insertion. *J. Mater. Chem.* **2011**, *21*, 11296–11305.
- (29) Needham, S. a.; Wang, G. X.; Konstantinov, K.; Tournayre, Y.; Lao, Z.; Liu, H. K. Electrochemical Performance of Co₃O₄-C Composite Anode Materials. *Electrochem. Solid-State Lett.* **2006**, *9*, A315–A319.
- (30) Schweikert, N.; Hahn, H.; Indris, S. Cycling behaviour of Li/Li₄Ti₅O₁₂ cells studied by Electrochemical impedance spectroscopy. *Phys. Chem. Chem. Phys.* **2011**, *13*, 6234–6240.
- (31) Gao, F.; Tang, Z. Kinetic behavior of LiFePO₄/C cathode material for Lithium-ion batteries. *Electrochim. Acta* **2008**, *53*, 5071–5075.
- (32) Kim, J. K.; Manuel, J.; Chauhan, G. S.; Ahn, J. H.; Ryu, H. S. Ionic liquid-based Gel polymer electrolyte for LiMn_{0.4}Fe_{0.6}PO₄ cathode prepared by Electro spinning technique. *Electrochim. Acta* **2010**, *55*, 1366–1372.
- (33) Huang, S.-Z.; Cai, Y.; Jin, J.; Li, Y.; Zheng, X.-F.; Wang, H.-E.; Wu, M.; Chen, L.-H.; Su, B.-L. Annealed Vanadium oxide Nanowires and Nanotubes as High performance Cathode Materials for Lithium ion batteries *J. Mater. Chem. A* **2014**, *2*, 14099–14108.
- (34) Doherty, C. M.; Caruso, R. a.; Smarsly, B. M.; Drummond, C. J. Colloidal Crystal Templating to Produce Hierarchically Porous LiFePO₄ Electrode Materials for High Power Lithium Ion Batteries *Chem. Mater.* **2009**, *21*, 2895–2903.
- (35) Liu, W. L.; Tu, J. P.; Qiao, Y. Q.; Zhou, J. P.; Shi, S. J.; Wang, X. L.; Gu, C. D. Optimized Performances of Core-shell structured LiFePO₄/C Nanocomposite *J. Power Sources* **2011**, *196*, 7728–7735.

TOC graphic



TOC graphic

